

Received January 13, 2020, accepted January 22, 2020, date of publication February 3, 2020, date of current version February 12, 2020.

Digital Object Identifier 10.1109/ACCESS.2020.2971038

# Neutralization Line Decoupling Tri-Band Multiple-Input Multiple-Output Antenna Design

RUIPENG LIU<sup>1,2</sup>, XING AN<sup>1</sup>, HONGXING ZHENG<sup>1,2</sup>, (Senior Member, IEEE),  
MENGJUN WANG<sup>1,2</sup>, ZHENBIN GAO<sup>2</sup>, AND ERPING LI<sup>1,3</sup>, (Fellow, IEEE)

<sup>1</sup>State Key Laboratory of Reliability and Intelligence of Electrical Equipment, Key Laboratory of Electromagnetic Field and Electrical Apparatus Reliability of Hebei Province, School of Electrical Engineering, Hebei University of Technology, Tianjin 300401, China

<sup>2</sup>School of Electronics and Information Engineering, Hebei University of Technology, Tianjin 300401, China

<sup>3</sup>University of Illinois at Urbana-Champaign Institute, Zhejiang University, Haining 314400, China

Corresponding author: Hongxing Zheng (hxzheng@hebut.edu.cn)

This work was supported in part by the National Natural Science Foundation of China, and in part by Natural Science Foundation through the Key Project of Hebei Province under Grant 61671200 and Grant F2017202283.

**ABSTRACT** A pair of tri-band multiple-input-multiple-output (MIMO) antennas with high isolation is investigated in this paper. The proposed antenna consists of two monopole antenna elements with an edge to edge spacing of 4 mm ( $0.03 \lambda_0$  at 2.3 GHz). The monopole antenna element chose the bending line structure that can operate in tri-band and realize miniaturization. To achieve compact dimension and high isolation, symmetrical distribution layout is adopted to decouple the low frequency band, the U-shaped neutralization line (NL) contacting with two microstrip lines, and it can to improve the isolation in high frequency band, and the inverted U-shaped NL contacting with two radiation patch can decoupling in the middle frequency band. And then study the envelope correlation coefficient is lower, and the radiation pattern in operation bands is quasi-omnidirectional. It indicates that the antenna has obtained a satisfactory diversity performance within the whole operation bands which can be a good candidate for some portable MIMO applications.

**INDEX TERMS** Multiple-input-multiple-output, tri-band, high isolation, neutralization line.


## I. INTRODUCTION

Multiple-input-multiple-output (MIMO) antennas have constantly captured wildly attention in the advances of the wireless communication, due to its outstanding advantages such as increased system capacity, diversity gain (DG), decrease envelope correlation coefficient (ECC) and so on. However, when the antenna elements are placed at closed space, mutual coupling deteriorates the performance of the MIMO system [1], [2].

Consequently, in order to improve the isolation, the antenna size and the distance between elements should be considered. As we all known that improving the isolation between antenna elements is significant for the MIMO antenna. For the single band antenna, we can use the decoupling network to improve isolation [3], [4]. At the same time, the negative effects of the traditional decoupling network are compensated by adding lumped elements to the parity-mode impedance converter. The periodic structure like electromagnetic band

gap structure is used to reduce the coupling between the MIMO antenna elements [5]–[7], but some structures are complicated and difficult to fabricate. Defected ground structure can effectively improve the isolation of the multi-band MIMO antenna [8]–[12]. For example, loading two winding structures on the ground plane, which can effectively reduce the coupling between dual-band antennas. However, attention the defected ground structure mainly affects the backward radiation pattern of the antenna.

But for the decoupling in the mutli-band MMO antenna, it has challenges. In order to realize the miniaturization and compactness, adding neutralization line (NL) on the MIMO antenna radiation elements is effective [13]. This structure has not affected the origin element structure, and can realize miniaturization. And also, it can take into account both the decoupling of the lower and high frequency band. The neutralization line technique is similar to the way of stub-loaded in MIMO antenna decoupling [14], except that the antennas are physical connection by neutralization line introducing a suitable the current (include magnitude and phase) from one antenna to nearby antenna and providing 180 phase

The associate editor coordinating the review of this manuscript and approving it for publication was Yasar Amin .

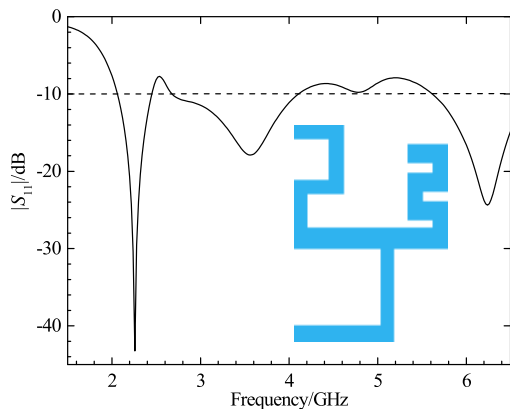


FIGURE 1. The simulated  $|S_{11}|$  of the monopole tri-band MIMO antenna element.

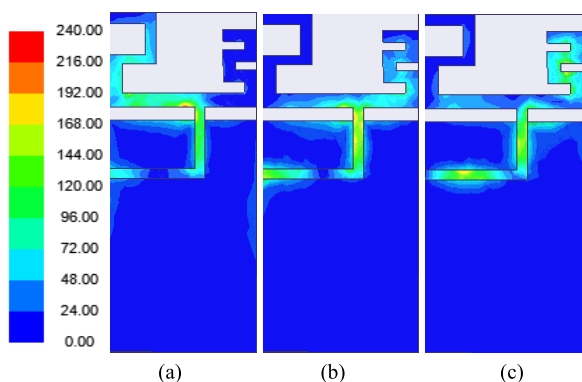


FIGURE 2. The current distributions of tri-band MIMO antenna element (unit: A/m), (a) 2.3 GHz, (b) 3.5 GHz, (c) 5.7 GHz.

shift to cancel out the existing coupling of two feeding ports [15], [16].

In order to reduce the size and complexity of the antenna. The antenna elements adopt a multi-branch winding structure, and layout uses symmetrical structure for realizing miniaturization and compact. We add the U-shape and inverted U-shaped NLs on the radiation patch, and it achieves tri-band decoupling.

The rest of this paper is as follows. Section II presents the structure of the proposed MIMO antenna and the element. Section III analysis the working mechanism of the two NLs, Section IV gives the measured results. Section V summarizes the conclusion about the all work.

## II. ANTENNA STRUCTURE DESIGN

### A. TRI-BAND MONOPOLE ANTENNA ELEMENT

The proposed MIMO antenna evolves from a compact tri-band monopole antenna. The two branches can make the antenna work in three bands at the center frequency of 2.3 GHz, 3.5 GHz and 5.7 GHz as shown in Figure 1.

The current distributions in three operation frequencies band are shown in Figure 2. We can find that the majority of the currents flow along the left branch at 2.3 GHz and the right branch can excite two resonance modes at 3.5 GHz

and 5.7 GHz, respectively. The width of the microstrip line is 1.5 mm. The length of the left, bottom and right side branches are 34.8 mm, 20.5 mm and 18.9 mm, respectively, which are approximately a quarter wavelength for 2.3 GHz, 3.5 GHz and 5.7 GHz, respectively.

The following analytical formula was used as an original rule to determine the lengths of monopole antenna operated at three frequency points [17]:

$$f_i = \frac{c}{4L'_i}, \quad i = 1, 2, 3. \quad (1)$$

where

$$L'_1 = W_1 + L_1 + 2L_2 + L_3 - W_3 - W_4. \quad (2)$$

$$L'_2 = W_1 + W_2. \quad (3)$$

$$L'_3 = 5L_5 - 5W_5 + L_4 - W_3. \quad (4)$$

$L'_1, L'_2,$  and  $L'_3$  stand for the approximated length of current trace operating at 3.5 GHz and 5.7 GHz.  $c$  is the free-space velocity of light.

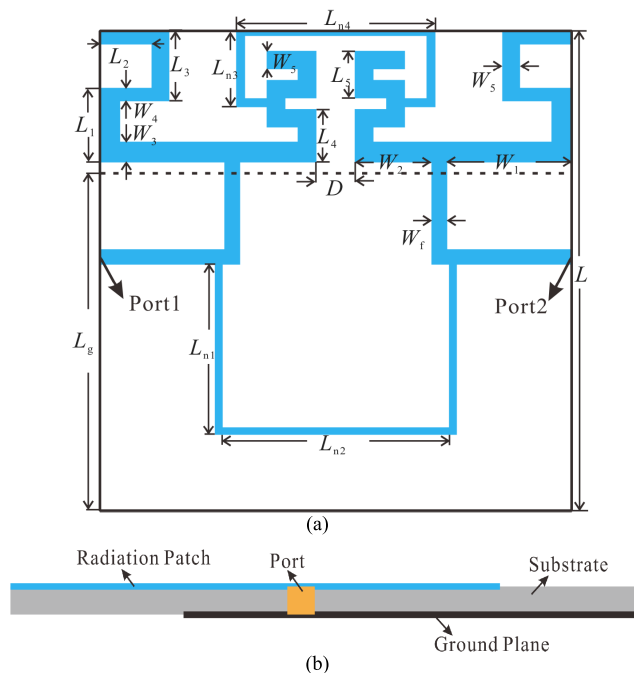


FIGURE 3. The structure of proposed antenna, (a) top view, (b) side view.

### B. THE MIMO ANTENNA CONFIGURATION

The proposed MIMO antenna consists of two symmetrical monopole tri-band antenna elements as shown in Figure 3, fed by microstrip lines through port1 and port2, respectively. Each monopole antenna elements possesses two meandered branches printed on the front side of the substrate for reducing the size of antenna. The edge to edge distance of two elements is only 4 mm ( $0.03 \lambda_0$  at the center frequency of 2.3 GHz). The U-shaped NL add on the microstrip feeder line of the antenna and inverted U-shaped NL contacts with two radiation elements.

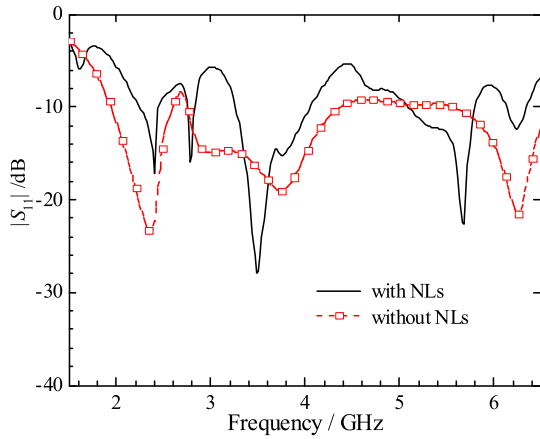


FIGURE 4. The simulated  $|S_{11}|$  with and without NLs.

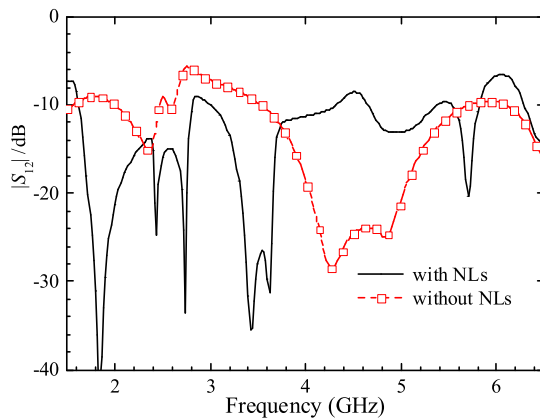


FIGURE 5. The simulated  $|S_{12}|$  with and without NLs.

The design of the decoupling network structure is more complicated [4], especially for multi-bands. The periodic structure [5] will increase the antenna profile and make it difficult to achieve miniaturization. This paper, the antenna elements adopts the multi-branch winding structure to miniaturization, and the structure of NLs is simple and it can achieve good decoupling performance.

### III. WORKING MECHANISM OF THE TWO NLs

To gain insight into the proposed antenna, working mechanism of the two NLs is analyzed based on the S-parameters, a simplified equivalent mode, and the surface current distributions. The effects of the parameters of the NLs on the broadband decoupling are studied step by step.

#### A. S-PARAMETERS OF THE MIMO ANTENNA WITH TWO NLs

Firstly, the scattering parameters  $|S_{11}|$  and  $|S_{12}|$  without and with NLs are also provided. The simulated results show that the coupling coefficient can be reach  $-25$  dB at center frequency while keeping good impedance matching as shown in Figure 4 and Figure 5. Simultaneously, it is shown that adding the NLs will degrade bandwidth and impedance at low frequency and high frequency. It is mainly due to a large

part of the NLs is added on the radiation patch, which will enlarge the inductance between the ground and NLs. So, it is inevitable that adding the decoupling structure can influence the performance of the MIMO antenna. The different combinations can conduce different Q values, and then the Q value can affect the isolation and bandwidth. The Q value of the NLs is given by the following equation:

$$Q = \sqrt{\frac{L}{C}}/R \tag{5}$$

where  $R$ ,  $L$ , and  $C$  are the internal resistance, inductance, and capacitance of the NLs. Adding the inductive component to elements and lead to a larger  $L$ . From (5), we can learn that the Q-factor of MIMO antenna elements will slightly enlarge and in turn lead to narrower bandwidth. However, the bandwidth of the proposed MIMO antenna can still successfully cover the lower band and high band.

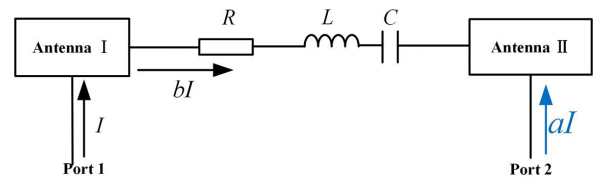


FIGURE 6. Equivalent model of the proposed antenna.

#### B. SURFACE CURRENT DISTRIBUTION OF THE MIMO ANTENNA WITH TWO NLs

There is the equivalent model of the decouple structure as shown in Figure 6. The length of the line specifies its inductance and its width specify its capacitance behavior. As antenna I is excited by current  $I$ , the coupled current  $aI$  can be appeared on the antenna II. To cancel out the coupling, the current  $bI$  is induced to the NLs. And the different combinations result in different  $bI$ . So to achieve the high isolation, the current  $aI$  and  $bI$  should be fine-tuned to fulfill the following equation

$$aI + bI = 0. \tag{6}$$

In this case, the NLs can act as band stop filter, effective filtering the current coupled to nearby antenna at specific frequency. Each of line corresponds to one of the decoupling frequency.

Due to distance of the two closely spaced antenna is only 4 mm and much less than one wavelength causing strong mutual coupling between two antenna elements, is inevitable, especially for the lower frequency band. For the 2.3 GHz, we first considered the layout of the antenna. The bending line structure are placed for the type of “back to back”, which is conducive to improving the isolation between elements in the lower frequency band. Then, put the meandered line structure operating at low frequency on both ends of the dielectric substrate to increase the ratio of  $D$  and  $\lambda_g$  ( $D$  denotes the distance between the antennas,  $\lambda_g$  denotes the working wavelength in the low frequency band) in limited space and therefore

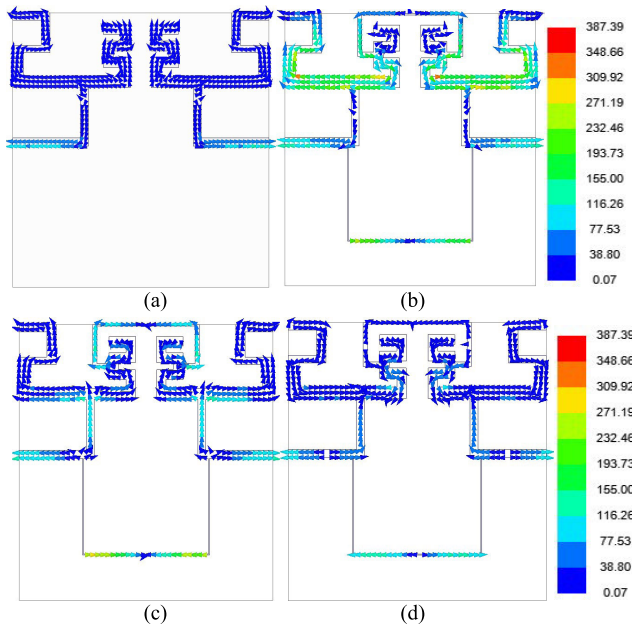


**FIGURE 7.** The current distribution of the proposed antenna (unit: A/m), (a) without NLs at 2.4 GHz, (b) with NLs at 2.4 GHz, (c) with NLs at 3.5 GHz and (d) with NLs at 5.7 GHz.

reduce the near-field coupling. According to the current distribution with and without the NLs, it can be seen that it has almost no effect between two antenna elements as shown in Figure 7 (a) and (b).

The proximal placement causes near-field coupling at 3.5 GHz and 5.7 GHz and increases the insertion loss between the feeding ports, therefore degrades the overall diversity performance of the two-antenna system. To compensate for this effect while maintaining a compact enough size and no modify the ground plane, a U shaped and inverted U-shaped NLs connecting two antenna elements from feed line and branch respectively are applied for the proposed MIMO antenna.

The length of the U-shaped NL is approximately one wavelength at the center frequency 5.7 GHz and the horizontal length of the inverted U-shaped NL is approximately half wavelength at the center frequency 3.5 GHz. We give the current distribution of designed MIMO antenna as shown in Figure 7(c) and (d). It indicates that the lines provide 180 phase shifts from the current fed to the nearby antenna. That is to say it excited corresponding resonant mode and allows two possible decoupling current paths with different lengths to cancel the coupling current near field. The detailed dimensions of decoupling structure, such as the length and width of NLs will be discussed in the next section.

To verify the effectiveness of the antenna design method, the current distributions of the proposed MIMO antenna with and without NLs are illustrated in Figure 8 to demonstrate the effectiveness of the decoupling. In the simulation, one antenna is excited while the other antenna is terminated by a  $50 \Omega$  load. Without the NLs, considerable current is coupled

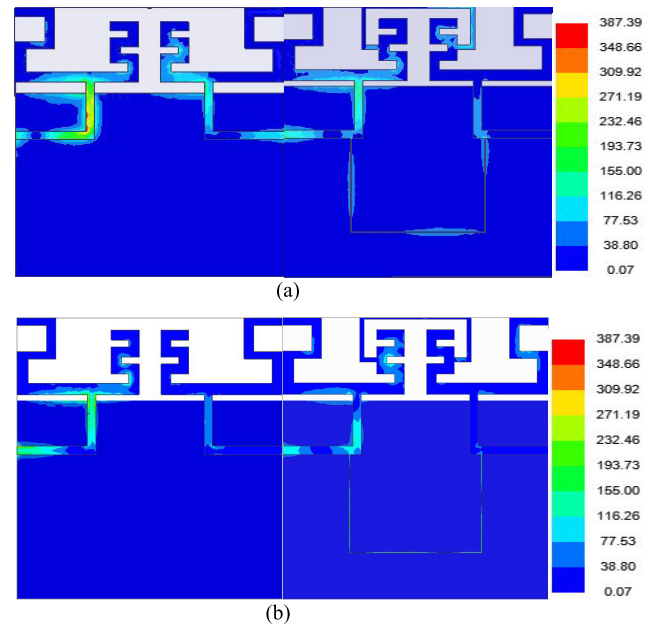


**FIGURE 8.** The current distributions of the proposed antenna (unit: A/m), (a) with and without NLs at 3.5 GHz, and (b) with and without NLs at 5.7 GHz.

to the adjacent antenna at 3.5 GHz, as shown in Figure 8(a). However, after adding the NLs, current of coupling mainly focused on the U-shaped inductive line with large inductive impedance. Although the distance between them is only 4 mm, the coupling current in the other antenna element is obviously reduced. At this moment the inverted U-NL is exactly in a resonant state, greatly improving the isolation of the middle frequency band.

Similarly, the NLs are in a state of resonance exactly, adding this decoupling structure, the coupling current between the two “bows” branches is obviously reduced. The inverted U-shaped NL reduce the coupling of two radiation patch at the middle frequency and the U-shaped NL connecting with the microstrip lines achieves the high isolation at the high frequency band as shown in Fig 8(b). It should be noted that after adding the NLs structure, the coupling current on the adjacent antennas is increased and the coupling between the two ports is increased, which is attributed to the extra current path it created.

### C. PARAMETER STUDY AND DISCUSSION

In order to further evaluate the effects of decoupling structure, parameter studies are carried out for the length of NLs. Firstly, the U-shaped NL (NL1) links to the feeder of two microstrip lines. The  $S$ -parameters with different NL  $L_{n1}$  and  $L_{n2}$  are presented in Figure 9. It is observed that with  $L_{n1}$  changing from 16.7 mm to 17.5 mm, the highest decoupling frequency moves to lower frequency band while the influence on the low frequency part is almost negligible. And also, the value of  $L_{n1}$  becomes smaller, the decoupling is improved more significantly, and also it has little influence at 2.3 GHz. Because the

TABLE 1. Dimensions of the proposed MIMO antenna (Unit: mm).

Dimension	$L$	$W$	$L_g$	$W_f$	$L_f$	$L_1$	$L_2$	$L_3$	$L_4$	$L_5$
Size	49	48	35	1.5	10.6	7.6	5.3	7.2	5.4	4.8
Dimension	$L_{n1}$	$L_{n2}$	$L_{n3}$	$L_{n4}$	$W_1$	$W_2$	$W_3$	$W_4$	$W_5$	$D$
Size	17.3	24	8.1	20.2	12.7	7.8	2	1.3	1.7	4

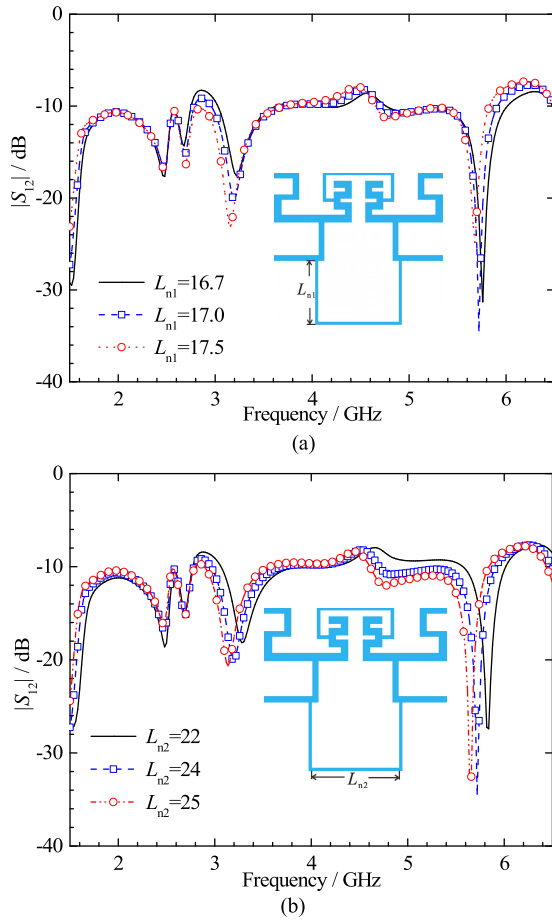


FIGURE 9. The simulated  $|S_{12}|$  with different length of  $L_{n1}$  and  $L_{n2}$ , (a) is  $L_{n1}$  with different size and (b) is  $L_{n2}$  with different size.

smaller  $L_{n1}$  is closer to the effective length corresponding to the decoupling frequency, and it leads to a higher decoupling current density on the suspended line, thereby the decoupling field is stronger. The parameter  $L_{n2}$  has similar effect on the performance of reducing the mutual coupling as shown in Figure 9(b). According to the above results, the optimal size of  $L_{n1}$  and  $L_{n2}$  are 17.3 mm and 24 mm, respectively.

Then, we give the  $S$ -parameters of the original and decoupled array as shown in Figure 10. It can be seen clearly that the isolation is improved considerably and there is a minimum 14 dB improvement on the isolation over the desired operating frequency band (5.54-5.79 GHz).

Also, we study the effect of the inverted U-shaped NL (NL2). The analysis of the parameters with  $L_{n3}$  and  $L_{n4}$  are given in Figure 11. As the value of  $L_{n3}$  or  $L_{n4}$  increases, the  $|S_{12}|$  decreases at the center frequency while higher cen-

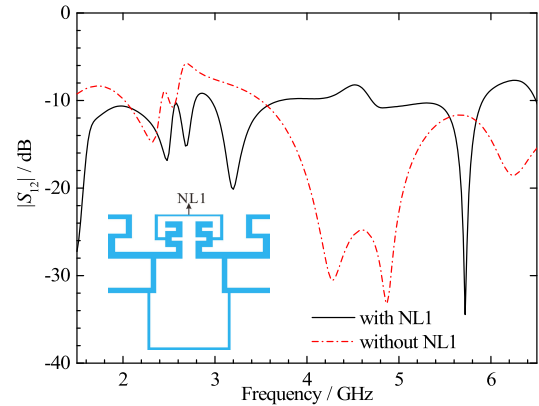


FIGURE 10. The simulated  $|S_{12}|$  with and without NL1.

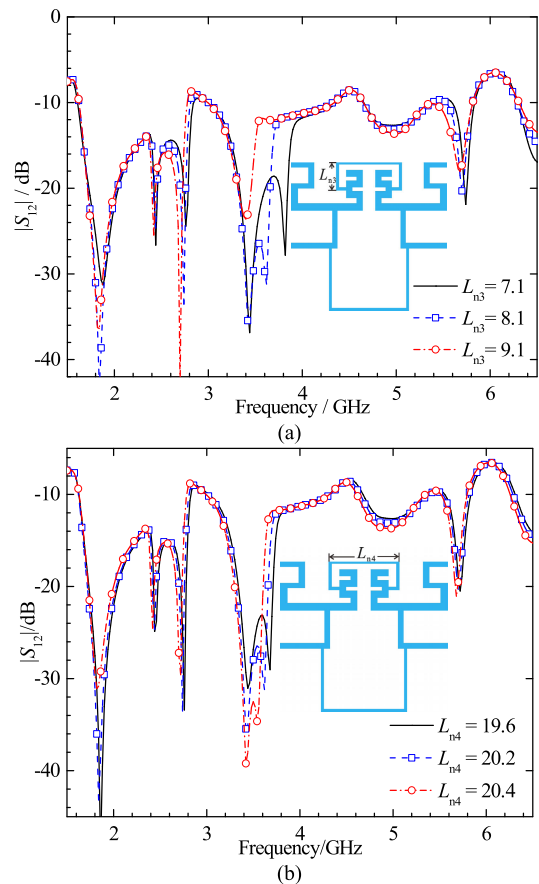


FIGURE 11. The simulated  $|S_{12}|$  with different length of  $L_{n3}$  and  $L_{n4}$  (a) is  $L_{n3}$  with different size and (b) is  $L_{n4}$  with different size.

ter frequency keeps low. With flexibly controlled NL2, the degree of decoupling freedom in middle frequency band is added. Also, we can observe that when the value of  $L_{n3}$

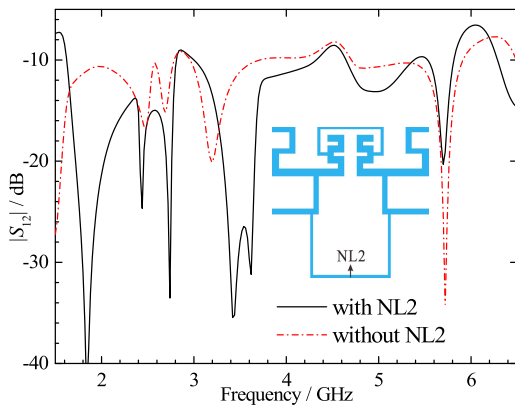


FIGURE 12. The simulated  $|S_{12}|$  with and without NL2.

or  $L_{n4}$  are fixed at 8.1 mm and 20.2 mm, the isolation of center frequency can reach up to  $-30$  dB and there is a minimum 14 dB improvement on the isolation over the desired operation frequency band (3.4-3.484 GHz). The isolation of multiband has been improved as shown in Figure 12.

Furthermore, the radiation patterns of antenna in the three bands were also simulated (antenna I is excited, while antenna II is terminated with a  $50 \Omega$  load) as shown in Figure 13. The simulation results show that antenna array has similar dipole radiation pattern. The directional diagram of H-plane in 2.3 GHz, 3.5 GHz, and 5.7 GHz is nearly circular and able to meet the radiation characteristics of monopole antenna. As the changing of the angle, E-plane turns into dumb-bell type and meets the bidirectional feature. On the whole, the fact that two elements possess complementary radiation patterns guarantees they can receive the signals from all directions which are suitable for wireless communications.

#### IV. EXPERIMENT RESULTS

According to the above analysis of the antenna structure, and reasonably adjust the parameters of the two NLs, improved about 14 dB in the whole operation band in the mutual coupling between two elements have been achieved. We chose the FR4 with dielectric constant of 4.4, loss tangent 0.02, thickness of 0.8 mm to design and fabricate the MIMO antenna. The simulation is processed by HFSS software. The optimal dimensions of the antenna are listed in table 1.

To verify the proposed decoupling method, Measurement environment and a fabricated prototype of tri-band MIMO antenna is shown in Figure 14. The S-parameters of the fabricated antenna are measured and also compared to the simulated results, as shown in Figure 15. The measured results are obtained when port 1 is excited and port 2 is terminated with a  $50 \Omega$  load. As we can see, the measured and simulated results are in good agreement. In the operation band (2.24-2.45 GHz, 3.3-4 GHz and 5.6-5.75 GHz), the  $|S_{11}|$  is below  $-10$  dB and  $|S_{12}|$  is lower than  $-15$  dB. There is good agreement between the simulated and measured radiation patterns. The H-planes for all resonant frequencies are all mostly omnidirectional, whereas the E-planes vary according to the resonant frequencies as shown in Figure 16.

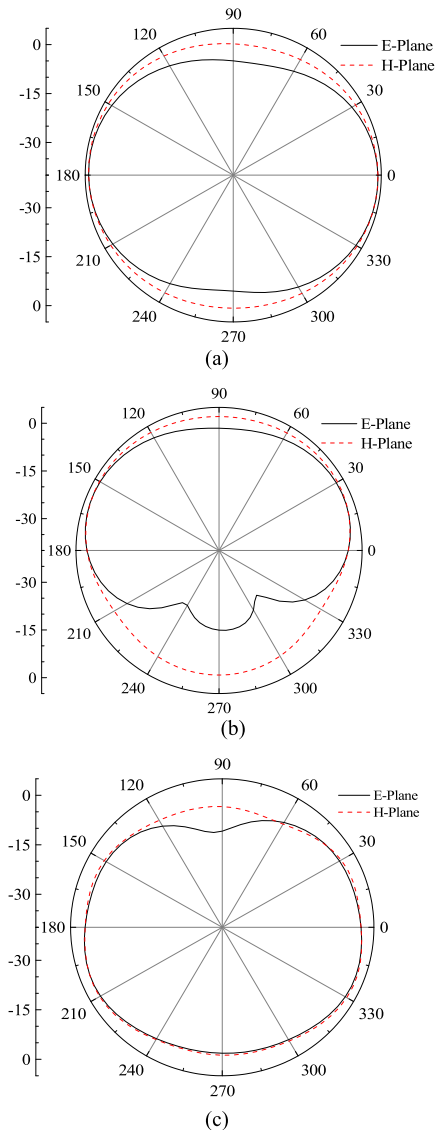


FIGURE 13. The radiation pattern of the proposed antenna with different resonant frequency, (a) 2.3 GHz, (b) 3.5 GHz and (c) 5.7 GHz.

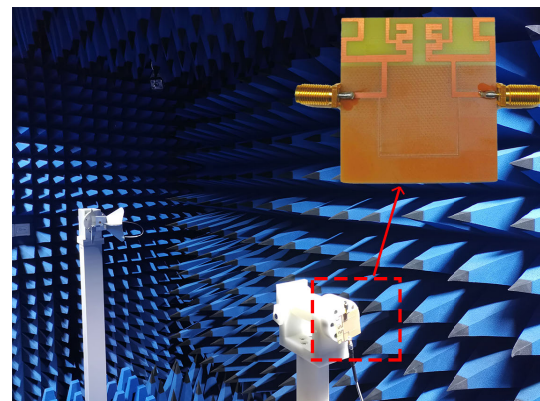


FIGURE 14. Measurement environment and the photograph of fabricated tri-band MIMO antenna.

In addition, good isolation does not exactly represent low mutual coupling. The mutual coupling involves the electromagnetic interaction between antennas, and ports isolation

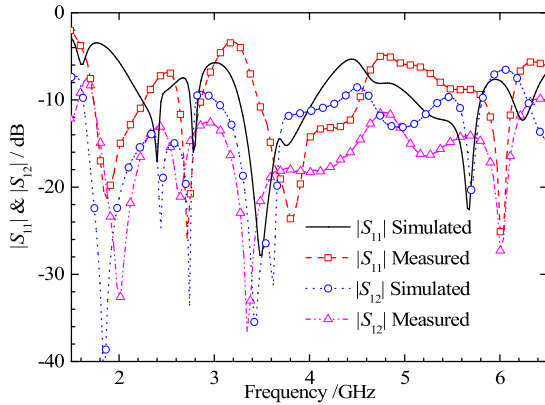


FIGURE 15. The simulated and measured S-parameters of the proposed antenna.

TABLE 2. Comparison of the proposed NL structure and other decoupling structure.

Reference	Operation frequency (GHz)	Edge-to-edge distance	Isolation (dB)
[4]	4.2	$0.23\lambda_0$	22
[10]	3.7	$0.034\lambda_0$	28.4
[13]	2.5	$0.04\lambda_0$	42.1
This work	2.3		18.2
	3.5	$0.03\lambda_0$	32.4
	5.7		24.3

just indicates the signal interference from one port to another port [18]. So to further understand the uncorrelated channels, studied the diversity performance of antenna. It can be evaluated by the ECC and DG. In the terms of isotropic/uniform signal propagation environments, the ECC involved in all the S-parameters can be calculated by using the following equation [19]:

$$ECC = \frac{|S_{11} * S_{12} + S_{21} * S_{22}|^2}{(1 - |S_{11}|^2 - |S_{21}|^2)(1 - |S_{12}|^2 - |S_{22}|^2)} \quad (7)$$

In general, to obtain the good diversity behavior, the correlation coefficient between MIMO antenna elements of mobile terminal equipment is less than 0.5. The better diversity performance is, the lower ECC is and vice versa. As shown in Figure 17, the ECC is lower than 0.02 across the operating bands in both simulation and measurement which indicates that the design of antenna has good pattern diversity. Besides, the DG is involved in the correlation coefficient, which is obtained in terms of ideal condition ( $DG_0=10$  dB) and ECC [25]. The lower the mutual coupling is, the higher the DG is and vice versa. The method of using the ECC to calculate DG is given by using the equation as follows [20].

$$G_{DG} = 10 \times \sqrt{1 - ECC^2} \quad (8)$$

The simulated and measured DGs of the proposed antenna using (8) are illustrated in Figure 18. It can be observed that the antenna has the high diversity gain which is more than

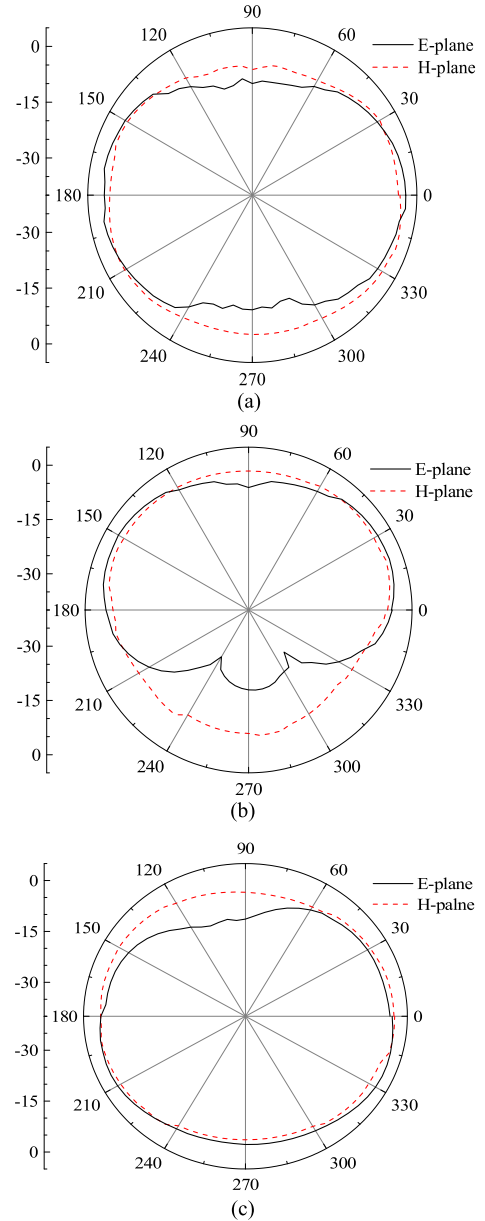


FIGURE 16. Measured results of the radiation pattern with different resonant frequency, (a) 2.3 GHz, (b) 3.5 GHz, and (c) 5.7 GHz.

9.9 dB within the frequency bands of interest. The antenna has a well channel characteristic. Overall, from the both key parameters (ECC and DG), the antenna has good performance of the diversity.

Table 2 shows the comparison of the proposed NL structure and other decoupling structure. In reference [4], the antenna structure is simple, the decoupling structure is complicated. This work proposed the U-shaped NL that the structure is simple and easy to fabricate. The proposed NL structure could base on the small edge-to-edge distance, achieve multi-bands decoupling, and also the isolation in the tri-bands is satisfied with design requirements.

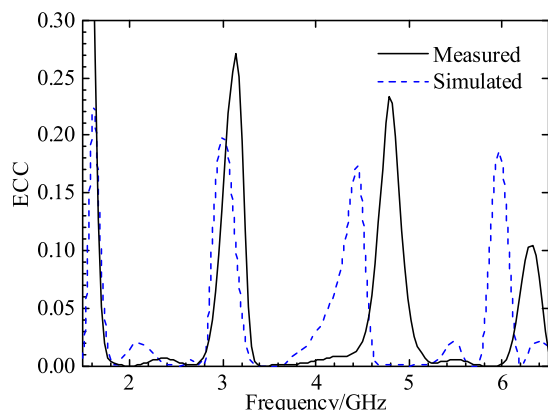


FIGURE 17. Measured and simulated ECC of the proposed antenna.

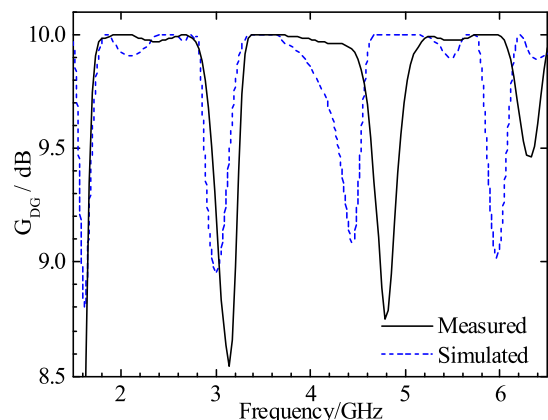


FIGURE 18. Measured and simulated DG of the proposed antenna.

## V. CONCLUSION

In this paper, a miniaturization and compact MIMO antenna is made up two tri-band monopole antennas with the multi-branch structure. Specially, symmetrical back to back structure can effectively improve the isolation in the low frequency band, and the elements edge-to-edge distance is only 4 mm, the U-shaped and inverted U-shaped NLs can be as the band stop filter, and they can decouple in the middle and high frequency bands. Through the measurement, the antenna can operate in the tri-band (2.24-2.45 GHz, 3.3-4 GHz and 5.6-5.75 GHz). The isolation has been substantially improved between the ports and the mutual coupling at the center resonant frequency of 2.3 GHz, 3.5 GHz and 5.7 GHz is less than  $-15$  dB,  $-30$  dB and  $-20$  dB, respectively. Furthermore, the radiation pattern at three resonance frequencies point are quasi-omnidirectional, the ECC is lower than 0.02 and the DG is closer 10, these performances indicates that the proposed antenna has a good application prospect in the multiband MIMO system.

## REFERENCES

- [1] S. Nandiwardhana and J.-Y. Chung, "Trade-off analysis of mutual coupling effect on MIMO antenna multiplexing efficiency in three-dimensional space," *IEEE Access*, vol. 6, pp. 47092–47101, 2018.
- [2] E. L. Bengtsson, F. Rusek, S. Malkowsky, F. Tufvesson, P. C. Karlsson, and O. Edfors, "A simulation framework for multiple-antenna terminals in 5G massive MIMO systems," *IEEE Access*, vol. 5, pp. 26819–26831, 2017.

- [3] M. Li, L. Jiang, and K. L. Yeung, "Novel and efficient parasitic decoupling network for closely coupled antennas," *IEEE Trans. Antennas Propag.*, vol. 67, no. 6, pp. 3574–3585, Jun. 2019.
- [4] Y.-M. Zhang, S. Zhang, J.-L. Li, and G. F. Pedersen, "A transmission-line-based decoupling method for MIMO antenna arrays," *IEEE Trans. Antennas Propag.*, vol. 67, no. 5, pp. 3117–3131, May 2019.
- [5] X. Tan, W. Wang, Y. Wu, Y. Liu, and A. A. Kishk, "Enhancing isolation in dual-band meander-line multiple antenna by employing split EBG structure," *IEEE Trans. Antennas Propag.*, vol. 67, no. 4, pp. 2769–2774, Apr. 2019.
- [6] Y. Liu, X. Yang, Y. Jia, and Y. J. Guo, "A low correlation and mutual coupling MIMO antenna," *IEEE Access*, vol. 7, pp. 127384–127392, 2019.
- [7] H. N. Chen, J.-M. Song, and J.-D. Park, "A compact circularly polarized mimo dielectric resonator antenna over electromagnetic band-gap surface for 5G applications," *IEEE Access*, vol. 7, pp. 140889–140898, 2019.
- [8] A. Ghalib and M. S. Sharawi, "TCM analysis of defected ground structures for MIMO antenna designs in mobile terminals," *IEEE Access*, vol. 5, pp. 19680–19692, 2017.
- [9] Z. Niu, H. Zhang, Q. Chen, and T. Zhong, "Isolation enhancement for  $1 \times 3$  closely spaced E-plane patch antenna array using defect ground structure and metal-vias," *IEEE Access*, vol. 7, pp. 119375–119383, 2019.
- [10] Z. Niu, H. Zhang, Q. Chen, and T. Zhong, "Isolation enhancement in closely coupled dual-band MIMO patch antennas," *IEEE Antennas Wireless Propag. Lett.*, vol. 18, no. 8, pp. 1686–1690, Aug. 2019.
- [11] R. Hussain, M. U. Khan, and M. S. Sharawi, "An integrated dual MIMO antenna system with dual-function GND-plane frequency-agile antenna," *IEEE Antennas Wireless Propag. Lett.*, vol. 17, no. 1, pp. 142–145, Jan. 2018.
- [12] S. F. Jilani and A. Alomainy, "Millimetre-wave T-shaped MIMO antenna with defected ground structures for 5G cellular networks," *IET Microw., Antennas Propag.*, vol. 12, no. 5, pp. 672–677, Apr. 2018.
- [13] C.-D. Xue, X. Y. Zhang, Y. F. Cao, Z. Hou, and C. F. Ding, "MIMO antenna using hybrid electric and magnetic coupling for isolation enhancement," *IEEE Trans. Antennas Propag.*, vol. 65, no. 10, pp. 5162–5170, Oct. 2017.
- [14] C.-Y. Hsu, F.-S. Chang, S.-M. Wang, C.-F. Liu, and L.-T. Hwang, "Investigation of a single-plate p-shaped multiple-input-multiple-output antenna with enhanced port isolation for 5 GHz band applications," *IET Microw., Antennas Propag.*, vol. 10, no. 5, pp. 553–560, Apr. 2016.
- [15] S. Zhang and G. F. Pedersen, "Mutual coupling reduction for UWB MIMO antennas with a wideband neutralization line," *IEEE Antennas Wireless Propag. Lett.*, vol. 15, pp. 166–169, 2016.
- [16] W. Hu, X. Liu, S. Gao, L.-H. Wen, L. Qian, T. Feng, R. Xu, P. Fei, and Y. Liu, "Dual-band ten-element MIMO array based on dual-mode IFAs for 5G terminal applications," *IEEE Access*, vol. 7, pp. 178476–178485, 2019.
- [17] A. Diallo, C. Luxey, P. Le Thuc, R. Staraj, and G. Kossiavas, "Study and reduction of the mutual coupling between two mobile phone PIFAs operating in the DCS1800 and UMTS bands," *IEEE Trans. Antennas Propag.*, vol. 54, no. 11, pp. 3063–3074, Nov. 2006.
- [18] S. Wang and Z. Du, "Decoupled dual-antenna system using crossed neutralization lines for LTE/WWAN smartphone applications," *IEEE Antennas Wireless Propag. Lett.*, vol. 14, pp. 523–526, 2015.
- [19] S. Zhang, Z. Ying, J. Xiong, and S. He, "Ultrawideband MIMO/diversity antennas with a tree-like structure to enhance wideband isolation," *IEEE Antennas Wireless Propag. Lett.*, vol. 8, pp. 1279–1282, 2009.
- [20] Z. Tang, X. Wu, J. Zhan, S. Hu, Z. Xi, and Y. Liu, "Compact UWB-MIMO antenna with high isolation and triple band-notched characteristics," *IEEE Access*, vol. 7, pp. 19856–19865, 2019.



**RUIPENG LIU** was born in Mengjin, China, in 1994. He received the B.S. degree in electronics engineering of the Distinguished Engineer Class from the Tianjin University of Technology and Education, Tianjin, China, in 2018. He is currently pursuing the M.S. degree in electronics science and technology with the Hebei University of Technology, Tianjin. He has published six articles in refereed journals and conference proceedings. He held four Chinese patents issued, in 2019. His current research interests include antennas and computational electromagnetics.





**XING AN** was born in Shijiazhuang, China, in 1992. She received the B.S. degree in communication engineering from the Hebei University of Science and Technology, Shijiazhuang, in 2016, and the master's degree in communication and information systems from the School of Electronics and Information Engineering, Hebei University of Technology, Tianjin, China, in 2019.

She is currently a Hardware Engineer with Ziguang Zhanrui Science and Technology Company, Ltd., Beijing, China. She is mainly engaged in radio frequency technology and millimeters wave technology.



**HONGXING ZHENG** (Senior Member, IEEE) received the Ph.D. degree in electronic engineering from Xidian University, Xi'an, in 2002.

He is currently a Professor with the School of Electronics and Information Engineering, Hebei University of Technology, Tianjin, China. He has authored six books and book chapters, and more than 200 journal articles and 100 conference papers. He held 45 Chinese patents issued, in 2019.

His recent research interests include wireless communication, design of microwave circuits and antennas, and computational electromagnetics. He is a Senior Member of the Chinese Institute of Electronics (CIE). He has received the Young Scientists Award presented by Tianjin Municipality, China, in 2008.



**MENGJUN WANG** was born in Hebei, China, in 1978. He received the B.S. degree in information engineering and the M.S. degree in physical electronics from the Hebei University of Technology, Tianjin, China, in 1999 and 2005, respectively, and the Ph.D. degree from Tianjin University, Tianjin, China, in 2008.

He is currently an Associate Professor with the School of Electronics and Information Engineering, Hebei University of Technology. His research interests include microwave radio frequency technology, flexible electronics devices, and electromagnetic compatibility.



**ZHENBIN GAO** received the B.S. degree in electrical engineering and the M.S. degree in semiconductor devices and microelectronics from the Hebei University of Technology, Tianjin, China, in 1995 and 1998, respectively, and the Ph.D. degree in signal and information processing from the Beijing Institute of Technology, Beijing, China, in 2005.

He is currently a Professor with the School of Electronics and Information Engineering, Hebei University of Technology. His research interests include realtime signal processing technology and electromagnetic compatibility in ICs.



**ERPING LI** (Fellow, IEEE) received the Ph.D. degree in electrical engineering from Sheffield Hallam University, Sheffield, U.K., in 1992.

From 1993 to 1999, he was a Senior Research Fellow, a Principal Research Engineer, an Associate Professor, and the Technical Director of Singapore Research Institute and Industry. In 2000, he joined the Singapore National Research Institute of High-Performance Computing, as the Principal Scientist and the Director of the Department of Electronic and Photonics. He also holds the post of Distinguished Professor with Zhejiang University. He has authored or coauthored more than 400 articles, published in various conference proceedings, and two books. His research interests include electrical modeling and design of micro/nano-scale integrated circuits, 3-D electronic package integration, and nano-plasmonic technology. He received numerous awards, including the IEEE Electromagnetic Compatibility Richard Stoddard Award for outstanding performance. He was the founding General Chair of Asia-Pacific EMC Symposium, in 2008, 2010, and 2012. He has been invited to deliver talks and plenary speeches at various international conferences and forums.

• • •